

Emerging deep learning techniques using magnetic resonance imaging data applied in multiple sclerosis and clinical isolated syndrome patients (Review)

ELEFThERIOS E. KONTOPODIS^{1,2}, EFROSINI PAPADAKI^{1,2}, ELEFThERIOS TRIVIZAKIS^{1,2}, THOMAS G. MARIS^{1,2}, PANAGIOTIS SIMOS^{1,3}, GEORGIOS Z. PAPADAKIS^{1,2}, ARISTIDIS TSATSAKIS⁴, DEMETRIOS A. SPANDIDOS⁵, APOSTOLOS KARANTANAS^{1,2} and KOSTAS MARIAS^{1,6}

¹Computational BioMedicine Laboratory, Institute of Computer Science, Foundation for Research and Technology-Hellas; Departments of ²Radiology and ³Psychiatry and Behavioral Sciences, Medical School, University of Crete, 70013 Heraklion; ⁴Centre of Toxicology Science and Research, Faculty of Medicine; ⁵Laboratory of Clinical Virology, Medical School, University of Crete, 71003 Heraklion; ⁶Department of Electrical and Computer Engineering, Hellenic Mediterranean University, 71410 Heraklion, Greece

Received April 12, 2021; Accepted July 29, 2021

DOI: 10.3892/etm.2021.10583

Abstract. Computer-aided diagnosis systems aim to assist clinicians in the early identification of abnormal signs in order to optimize the interpretation of medical images and increase diagnostic precision. Multiple sclerosis (MS) and clinically isolated syndrome (CIS) are chronic inflammatory, demyelinating diseases affecting the central nervous system. Recent advances in deep learning (DL) techniques have led to novel computational paradigms in MS and CIS imaging designed for automatic segmentation and detection of areas of interest and automatic classification of anatomic structures, as well as

optimization of neuroimaging protocols. To this end, there are several publications presenting artificial intelligence-based predictive models aiming to increase diagnostic accuracy and to facilitate optimal clinical management in patients diagnosed with MS and/or CIS. The current study presents a thorough review covering DL techniques that have been applied in MS and CIS during recent years, shedding light on their current advances and limitations.

Contents

1. Introduction
2. Selection criteria
3. Detection: Segmentation methods
4. Classification: Diagnosis
5. Post processing techniques and image enhancement methods
6. Discussion

Correspondence to: Dr Eleftherios E. Kontopodis, Computational BioMedicine Laboratory, Institute of Computer Science, Foundation for Research and Technology-Hellas, 100 Nikolaou Plastira Street, Vassilika Vouton, 70013 Heraklion, Greece
E-mail: lkontopodis@gmail.com

Abbreviations: MS, multiple sclerosis; CNS, central nervous system; BBB, blood brain barrier; CIS, clinically isolated syndrome; MRI, magnetic resonance imaging; CA, contrast agent; FLAIR, fluid-attenuated inversion recovery; CSF, cerebrospinal fluid; DWI, diffusion weighted imaging; AI, artificial intelligence; CAD, computer aided diagnosis; DL, deep learning; GM, gray matter; CNNs, convolution neural networks; NAWM, normal appearing white matter; NAGM, normal appearing gray matter; TPR, true positive rate; FPR, false positive rate; FCNN, fully convolutional neural network; AUC, area under curve; DBN, deep belief network; HC, healthy controls; PReLU, parametric rectified linear unit; LRP, layer-wise relevance propagation; NMOSD, neuromyelitis optical spectrum disorder; EDSS, expanded disability status scale; PET, positron emission tomography; MWF, myelin water fraction

Key words: magnetic resonance imaging/diagnosis, multiple sclerosis, deep learning, clinical isolated syndrome

1. Introduction

Multiple Sclerosis (MS) is a chronic inflammatory demyelinating disease of the central nervous system (CNS), commonly affecting young adults. MS usually manifests as a relapsing-remitting (RR) process, predominantly characterized by inflammatory demyelination that secondarily evolves to a progressive stage with neurodegeneration, gliosis and accumulating disability. Although the etiology of MS is largely unknown, it is considered primarily an autoimmune disease, in which activated myelin-specific T-cells, migrate from the periphery to the CNS, by crossing the blood brain barrier (BBB) inducing the formation of new inflammatory demyelinating lesions (1,2). Clinically isolated syndrome (CIS) describes a clinical episode of at least 24 h, suggestive of an inflammatory demyelinating disorder of the CNS. CIS usually

occurs in young adults and represents a monophasic episode, isolated in time, and usually isolated in space, affecting optic nerves, the brainstem, or the spinal cord, while there are no signs of fever or infection. Although patients usually recover from their presenting episode, CIS is often the first manifestation of MS. The course of MS after CIS is variable: after 15-20 years, one third of patients have a benign course with minimal or no disability, while half will have developed secondary progressive MS with increasing disability (3,4). MS and CIS clinical studies, need to be accompanied by sensitive and reliable imaging methods, in order to investigate the specific pathological alterations of the white matter (WM). Imaging methods for MS include optical computed tomography and coherent anti-Stokes Raman scattering microscopy (5). Magnetic Resonance Imaging (MRI) is the modality of choice for diagnosis and monitoring MS pathology, by exploiting both conventional and quantitative protocols (6).

Conventional MR techniques for MS and CIS imaging, include T1-w images since in this protocol lesions are usually depicted by lower signal intensity compared to the surrounding tissues, while T1 severe hypointense lesions (black holes) represent the most severe stage of MS lesions with irreversible axonal loss (5,7). Lesions in earlier stages of the disease can be captured using Gd enhanced T1-w MRI sequences, based on the fact that contrast agent (CA) uptake indicates premature stage of inflammation and blood brain barrier (BBB) disruption. Furthermore, T2-w MRI sequences are also sensitive in detecting lesions, since these are demonstrated as bright areas in a dark background. T2 hyperintense lesions represent tissues that are characterized by edema, inflammation, demyelination, axonal loss and gliosis. Sensitivity is further enhanced by using the fluid-attenuated inversion recovery (FLAIR) protocol, which can be used for highlighting subcortical and periventricular lesions by suppressing T2 signal from cerebrospinal fluid (CSF) (8). The aforementioned techniques constitute the gold standard for MS and CIS diagnosis and monitoring (9).

However, conventional MRI do not provide sufficient sensitivity that could enable early diagnosis or appropriate specificity to predict disease severity. Quantitative MRI techniques provide enhanced insights in disease severity and tissue damage. These techniques include: i) MR spectroscopy which provides a non-invasive method to examine the biochemical changes in MS (10); ii) magnetization transfer imaging which offers improved sensitivity and specificity for MS studies (11,12); iii) diffusion weighted imaging (DWI) and diffusion tensor imaging (DTI) which are quantitative MRI techniques, providing information on size, integrity, geometry, and orientation of tissue fibres by capturing the motion of tissue water (13); iv) dynamic contrast enhanced MRI which enables quantification of BBB disruption, a therapeutic target in MS (14); and v) dynamic susceptibility contrast MRI that provides quantitative maps of cerebral blood flow, cerebral blood volume and temporal parameters such as mean transit time by intravenous administration of CA (14).

Conventional clinical protocols for MS diagnosis and monitoring, utilize imaging data and measurements, such as signal intensities and volumetric results from user defined regions of interest, in order to compare healthy and MS subjects or to examine longitudinal changes during therapy, and evaluate the clinical outcome. However, these results are prone to errors

due to inter-observer variability, while the lack of ability to compare studies from different modalities is a major limitation. Moreover, procedures that involve human interplay, besides that are time consuming and employ human experts, these may be characterized by high inter observer variability that may hinder the quality of the final results. Therefore, during the last years artificial intelligence (AI) techniques have opened new horizons in computer aided diagnosis (CAD) systems, by automatically generalizing rules and patterns that exist in labeled imaging data, while by utilizing this information they are able to generate predictions and classifications on independent datasets that were not used in the model training process (15).

Furthermore, segmentation techniques in MS imaging are gaining ground during the last years, considering the necessity of accurate algorithms for automatic delineation of anatomical structures (16). Performing these tasks manually is time-consuming and prone to errors, thus there is a lot of interest to accomplish this task using automated computer algorithms, towards increased accuracy and precision, while at the same time minimize human involvement.

Finally, computer algorithms able to assess image quality of the acquired data, as well as methods that are able to compute optimal protocol parameters prior to image acquisition, are tools that can save time and provide noise free and qualitative data with increased diagnostic information (17). To this purpose, AI techniques constitute a valuable methodology for assessing MR image quality as well as determining the necessity to repeat the acquisition, while there are attempts to provide algorithms aiming to image protocol optimization.

The focus of this review paper, is to study the current literature regarding MR imaging deep learning (DL) applications focused on MS and CIS imaging. The reviewed publications were examined from different standpoints including the different DL architectures, the patient cohorts and the end-point of the reported studies in the field.

2. Selection criteria

Based on a PubMed search using keywords: ‘deep learning’ AND ‘multiple sclerosis’, 74 articles were initially identified. Subsequently, screening for MR imaging relevance and removing duplicates led to 32 original research articles that applied DL techniques in MS and CIS for diagnosis tasks, segmentation tasks and clinical protocol optimization. Afterwards, a similar search in google scholar, using the same keywords, and keeping only original research journal papers, led to 13 additional articles making a total of 45 original papers.

After an initial review, selected articles were separated in three broad categories i.e., i) segmentation of MS and CIS lesions; ii) classification of different pathologies and anatomical structures; and iii) post processing techniques and image enhancement methods with application in MS and CIS imaging. In Fig. 1 presents the general workflow of the DL techniques along with the final goal, as was determined in the present review manuscript. In Fig. 2, the distribution of the reviewed papers in each of the three abovementioned categories is presented. Obviously, segmentation and classification techniques are the main areas of interest, accounting for the

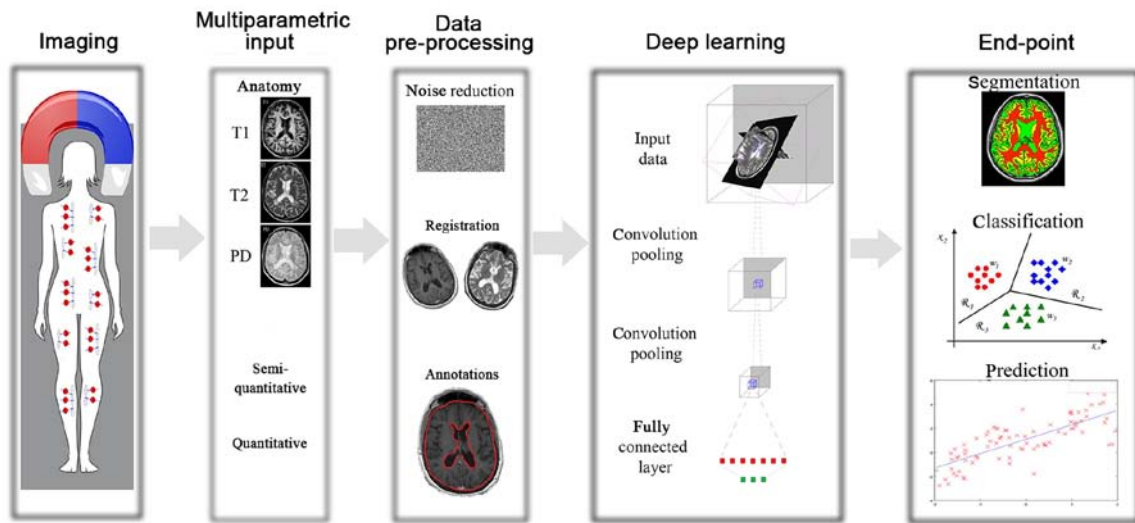


Figure 1. A schematic generalized workflow of the DL techniques presented in the manuscript. Initially the magnetic resonance acquisition is performed, producing a number of different anatomical and functional map representations. These provide additional information regarding the underlying pathophysiology (for example, quantitative), which can be used as input in the DL architecture for training the models and, in turn, address un-met clinical needs. DL, deep learning.

Distribution of publications through categories

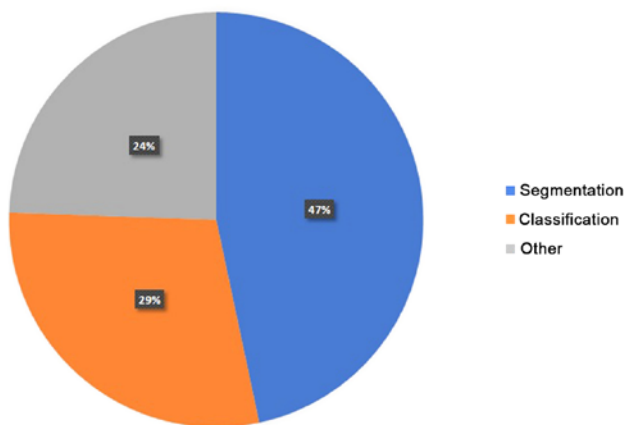


Figure 2. Pie chart distribution, grouping reviewed studies according to different end-points. The vast majority of published articles are serving segmentation and classification techniques.

76% of the overall publications. Moreover, in Fig. 3 the number of publications through years, for the three abovementioned application fields, is presented.

3. Detection: Segmentation methods

MS is a progressive disease of CNS affecting the myelin sheath, a fatty material that envelops neuron axons, and as a result alters the morphology and structure of the brain. Furthermore, brain atrophy is taking place in cortical and subcortical regions, whereas the gray matter (GM) atrophy and its association with disability and cognitive impairment is under investigation (18,19). Nevertheless, measurement of GM volume is a useful method for assessing the overall GM damage and can be estimated through conventional MRI techniques (6). Another established measurement for prediction of neurological disorders is the lesion load (20), since

it has been proved that both lesion volume and lesion count are strong predictors of disease course and progressive time-points. Additionally, detection of MS lesion is of paramount importance since the diagnosis of MS is based on the spatial and temporal distribution of focal demyelination lesions (21). Since manual detection of MS lesions is time consuming and prone to errors as well as inter observer variability, algorithms aiming to automatically delineate these tissues may constitute a great tool for clinical practice. Considering all the aforementioned, automated computer algorithms aiming to segment anatomical structures as well as to detect MS lesions, are valuable tools for clinicians offering objective and repeatable results. Accurate segmentation of WM lesions is hindered due to overlapping intensities of these lesions with GM, while finite resolution of MR images, complicated shapes that vary among different lesions as well as the partial volume effect, hamper the accurate delineation of MS tissues. Additionally, gray matter lesions are often not visible in T2-w images due to size, magnetic relaxation characteristics and partial volume effects with CSF. Finally, these lesions may not be visible even in FLAIR sequences, despite the increased sensitivity of this protocol compared to a conventional T2-w one.

Many previous studies have proposed DL methods aiming to provide a robust and reliable framework for detection and segmentation of MS lesions, while the most significant of are summarized below. Valverde *et al* (22) presented an automated WM lesions segmentation method, by utilizing a cascade of two 3D patch-wise convolution neural networks (CNN), the first was sensitive for revealing possible candidate lesions voxels while the second one was responsible for reducing the number of misclassified voxels resulted from the first network. The accuracy of the proposed approach was evaluated in the medical image computing and computer assisted intervention society (MICCAI) 2008 database (<http://www.ia.unc.edu/MSseg>), as well as on two private MS clinical datasets, while results were also compared with other lesion segmentation tools and methods. It was reported that the proposed

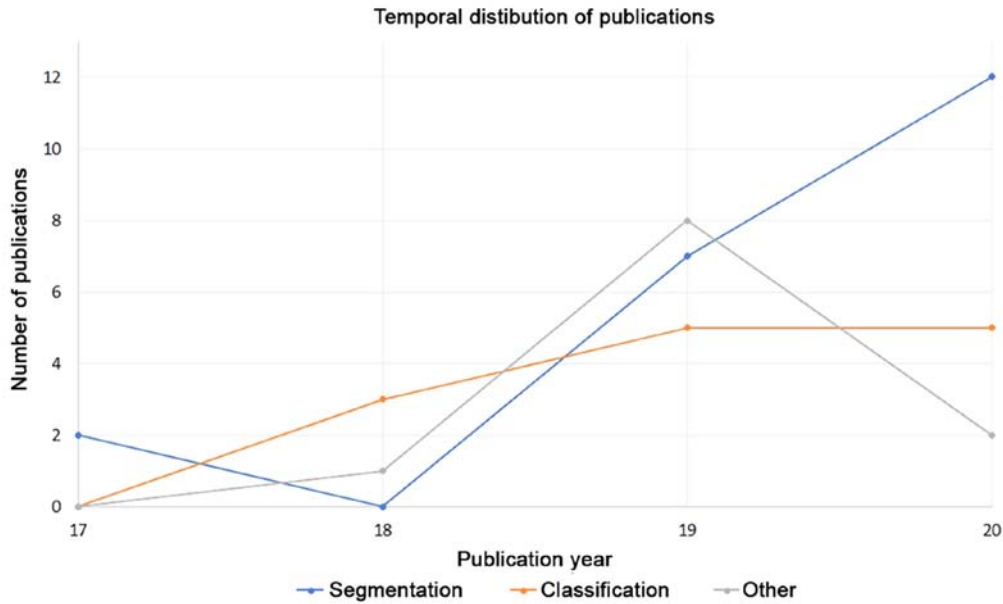


Figure 3. Number of publications, in each application category, per year. There is a trend indicating that the number of publications in the segmentation and classification categories are increasing in recent years.

approach is the best ranked on the MICCAI2008 challenge, and in the clinical datasets it exhibited an increased accuracy in the WM lesions segmentations.

Birendaum *et al* (23) developed an automated DL method for MS lesion segmentation, utilizing a CNN that was mainly based on the Single View CNN (V-Net) and the Longitudinal Network (L-Net). For this work, the 2015 Longitudinal MS Lesion Segmentation Challenge dataset (24) was used while the network resulted in Dice Similarity Coefficient 0.627. Finally, authors reported that the aforementioned method achieved performance level comparable to a trained human rater.

Gros *et al* (25), proposed a fully-automated framework for segmenting spinal cord and intramedullary MS lesions using conventional MRI data. The aim of this study was to provide a robust and automated framework, by overcoming the technical limitations of large variabilities related to acquisition parameters and image artifacts, and furthermore to eliminate the inter-rater variability as well as to optimize the large-throughput analysis pipeline. The cohort of this study consisted of 1,042 subjects; 459 healthy controls, 471 MS patients and 112 with other spinal pathologies. Authors used a sequence of two CNNs, the first intended for the detection of spinal cord centerline using 2D convolutions, while the second segmented the spinal cord and/or lesions using 3D convolutions. These networks were trained independently using the Dice loss (26), considering that it is not sensitive to high class imbalances, while comparing the proposed technique with the PropSeg method, an unsupervised technique for spinal cord segmentation (27), resulted in median Dice 95% when using manual vs 88% when using PropSeg. Moreover, regarding MS lesion segmentation, the proposed technique provided Dice of 60%, while sensitivity and precision were 83% and 77% respectively.

Aslani *et al* (28) presented an automated approach for MS lesion segmentation, based on a Deep end-to-end 2D CNN,

a technique that incorporates a multi-branch down-sampling path which enables the network to encode information stemming from multiple modalities in a separate way. The proposed model was trained and tested by using orthogonal plane orientations for every 3D modality, in order to exploit information from all directions. Evaluation of the proposed method was on two datasets, one private (37 MS patients) as well as the International Symposium on Biomedical Imaging (ISBI) 2015 longitudinal MS lesion segmentation challenge dataset (14 MS patients) (24). Results on the ISBI challenge ranked the proposed methodology among the top (DSC 0.6114), while on the private dataset the proposed method achieved the best results (DSC 0.6655).

Sander *et al* (29), employed a fully automated segmentation method, based on multi-dimensional gated recurrent units (MD-GRU). MD-GRU, is a DL approach that employs a convolutional adaptation of a recurrent neural architecture. This network was trained on 50 MS patients and 17 healthy controls, while a refinement procedure of the algorithm parameters took place in a cohort of 20 independent MS patients. For accuracy testing, 20 MS or CIS patients from the same cohort were used, while accuracy was further assessed in a dataset including 80 independent MS or CIS patients from the same cohort. Reproducibility assessment was followed by considering T1-w images from 33 healthy controls. Finally, robustness of the segmentation approach was assessed using images from 50 Alzheimer patients. According to the results, the proposed segmentation approach provided accurate, highly reproducible and a robust fully-automated segmentation framework for the brainstem and its substructure in both healthy controls as well as in MS and Alzheimer disease patients. In more detail, study results were compared with FreeSurfer (30) software results, while authors reported that the mean % change/SD between test-retest brainstem volumes were 0.45%/0.005 for MD-GRU and 0.95%/0.009 for FreeSurfer and 0.86%/0.007 for manual segmentations.

MD-GRU segmentations were compared to segmentations performed from experts, resulted in mean Dice score/SD of 0.97/0.005 for brainstem, 0.95/0.0131 for mesencephalon, 0.98/0.006 for pons and 0.95/0.015 for medulla oblongata.

Hashemi *et al* (31), developed a 3D fully connected convolution neural network (FCNN) with DenseNet blocks (FC-DenseNet), using an asymmetric similarity loss function Tversky index, aiming to mitigate the data imbalance problem and to achieve a better trade-off among precision and recall. This method used 15 patients from the MS lesion segmentation challenge (MSSEG) of the 2016 Medical Image Computing and Computer Assisted Intervention conference (32), as well as 5 patients from the longitudinal MS lesion segmentation challenge of the IEEE International Symposium on Biomedical Imaging (ISBI) conference (33). For training purposes, a 5-fold cross validation strategy was utilized, in which five instances of the training were performed on 4/5th of each dataset and validated on the remaining 1/5th. For testing the implemented architecture, due to limited number of subjects 5-fold cross validation was used. Study results report that MS lesion segmentation presented improved performance evaluation metrics by using asymmetry similarity loss function rather than using the Dice similarity in the loss layer. Furthermore, authors reported that the proposed framework achieved improved precision-recall trade-off and average DSC scores of 69.9% and 65.74% for MSSEG 2016 and ISBI longitudinal MS lesion segmentation challenge correspondingly.

Gabr *et al* (34) investigated the performance of FCNN in segmenting brain tissues using a larger cohort of MS patients. The MRI protocols and the patient cohort used in this study, included a dual echo fast spin echo (FSE) sequence, a T1-w sequence and FLAIR sequence from a cohort of 1,000 RRMS patients emanating from the CombiRx clinical trial, while training, validation and testing of the FCNN were based on the aforementioned data. Moreover, automated segmentation results were validated by two experts, while for cross-validation of the results, the leave-one-centre-out approach was used. Results from this study, report high average Dice similarity coefficient for all segmented tissues (0.95 for WM, 0.96 for GM, 0.82 for CSF and 0.82 for T2 lesions), and high correlations among the DL segmented tissues and the annotations from the expert ($R2 > 0.92$). Finally, cross validation reported consistency of the results among the different centers.

Weeda *et al* (35) compared four different lesion segmentation methods to investigate the suitability of the DL CNN method *nicMSLesions* (36), in an independent dataset aiming to determine whether this method is suitable for larger, multi-center studies. For this purpose, manual segmentation was performed in 14 MS subjects, while five different automated lesion segmentation methods were compared: i) unsupervised-untrained LesionTOADS (37); ii) supervised-untrained methods with threshold adjustment LST-LPA (38) and *nicMSLesions* with default settings; iii) supervised-untrained LST-LPA with threshold adjustment; iv) supervised-trained with leave-one-out cross-validation *nicMSLesions* and BIANCA (39); and v) supervised-trained on a single subject *nicMSLesions*. Results from this study report that the best volumetric and spatial agreement with manual annotations was obtained with the supervised and trained methods *nicMSLesions* and BIANCA, while the worst results

was provided by the unsupervised, untrained method LesionTOADS, concluding that input from a single subject to fine tune a DL CNN is sufficient for lesion segmentation.

McKinley *et al* (40) presented a segmentation framework based on a cascade of two CNNs, providing multimodal MR images segmentation into lesion, normal appearing white matter (NAWM) and normal appearing gray matter (NAGM) structures. For this purpose, MRI exams from 122 RRMS patients were used (90 patients for training and validation of the classifier, 32 patients for testing), while a second dataset including 10 MRI datasets was used for direct comparison with other centers. Results in the current study reported that both Dice coefficient as well as specificity and sensitivity are improved compared to previous approaches, while a good agreement with individual human raters was achieved. Moreover, authors concluded that the proposed method performed well on data emanating from different centers, scanners and field-strengths that were not represented in the training dataset indicating good generalizability, while it was also reported that the classifier achieved to identify lesions missed by human raters.

Narayana *et al* (41) studied the dependence of DL segmentation accuracy on the training size, aiming to define the required training set for an adequate accuracy in brain MRI segmentation in MS patients. For this purpose, a 2D FCNN was trained using 16 different training sizes, while segmentation accuracy was determined according to the training size, and network performance was evaluated by the dice similarity coefficient and lesion true-positive and false positive-rates. The presented methodology was evaluated in MRI data from a cohort of 1,008 MS patients, while the automatic segmentation results were assessed by two neuroimaging experts. Study results report that lesion segmentation showed stronger dependency to the sample size comparing with the GM, WM and CSF, concluding that excellent results were provided by a training set of 10 image volumes for GM, WM and CSF. Finally training size of at least 50 images was necessary for adequate lesion segmentation with DSC < 0.68 while for 150 sample size the DSC was 0.82.

Nair *et al* (42) presented a 3D MS lesion detection and segmentation CNN. The network was trained using a large scale, multi-site, multi-scanner clinical MS dataset consisted of 1,064 RRMS patients scanned annually over a period of 24 months, while imaging protocol included T2w, T1-w, FLAIR and proton density (PD) images. The network was trained using a weighted binary cross-entropy loss, while the performance of the network was evaluated separately in i) a voxel-level analysis; and ii) lesion-level analysis. Study results report that uncertainty filtering vastly improves lesion detection accuracy for small lesions.

In the same dataset, McKinley *et al* (43) trained two state-of-the-art CNNs architectures, a 3D Unet consisting a reference implementation and a more recently proposed architecture, the DeepSCAN, in order to segment multimodal MR images into lesion classes and NAWM and NAGM structures. Results from this study reported that both examined methods outperformed previous approaches in the literature related to the MSSEG dataset, while a good agreement among the automated segmentations and results from human raters is reported. Moreover, DeepSCAN network found to achieve

the best performance in both lesion and anatomical labelling, while there is reported that this classifier recognized lesions that were missed by human raters.

Narayana *et al* (44) investigated the effects that different combinations of multi-contrast MR images may infer when serving as input to a CNN. To this end, U-net, a fully CNN was used in order to automatically segment GM, WM, CSF and lesions in 1,000 MS patients. Image datasets included T1-w images, FLAIR and dual echo turbo spin echo or fast spin echo images. For the assessment of the segmentation performance, the DSC was evaluated, while for lesions the true positive rate (TPR) and false positive rate (FPR) were also reported. Results from this study report that when segmentation input was a combination of all four image modality data, it was achieved the highest DSC for all tissue volumes, while high DSC results were also obtained when FLAIR protocol was included in the segmentation input. Finally, it was reported that lesion segmentation was poor when considering very small lesions.

Salem *et al* (45), proposed a FCNN in order to detect early T2-w lesions in MR images. Patient cohort included 60 early MS and CIS patients, with a baseline and a follow-up study for each patient, while new T2-w lesions were found in the follow-up exam. Authors concluded that the proposed methodology achieved increased accuracy regarding the detected newly formed T2-w lesions, and therefore it has the potential to be used in the clinical practice for monitoring disease progression.

Brown *et al* (46) implemented a FCNN for automatic segmentation of orbital fat, tested on pediatric-inset MS patients, while they introduced a preprocessing step of image calibration aiming to remove technical intensity artefacts. This method was evaluated on 1,018 scans from 256 participants. Study results report that automatic segmentations agreed with manual segmentation from an expert, reporting estimated mean Jacard index 0.74, while the proposed image calibration contributed significantly in the performance of segmentation. Finally, the proposed methodology provided a robust serial calibration framework that allowed comparison of follow-up studies of the patient, while it is considered to be a fast technique that may be applied to large as well as to small datasets.

Ackaouy *et al* (47) proposed an unsupervised domain adaptation framework based on optimal transport (3D-U-net), Seg-JDOT, adapting a deep model to samples from a source domain to a target domain that share similar representations. This study used the MICCAI 2016 MS lesion segmentation challenge dataset (48) that contains 53 MRI images from MS patients, splitted to 15 train and 38 test images. Results from this study with single and multi-source training, indicated that model adaptation to a target site, can yield better model performance compared to the standard training.

Coronado *et al* (49) utilized a 3D CNN model based on multispectral MRI data of 1,006 RRMS patients, aiming to automatically segment gadolinium-enhanced T1 lesions. The dice similarity coefficient, true-positive rate, false-positive rate indexes over all the enhancing lesions were 0.77/0.90/0.23 when using FLAIR, T2 and pre- and post-contrast T1-w images, 0.72/0.86/0.31 when using only pre and post contrast T1-w images and comparable performance when using only post-contrast images.

La Rosa *et al* (50) proposed a framework for automatic segmentation of cortical and white matter lesions based on T1 and T2-weighted MRI data, in a cohort of 90 MS patients including 728 gray and 3,856 white matter lesions. For this purpose, an FCNN architecture based on the 3D-U-Net was used. Results of the present study reported that the proposed framework was able to achieve a detection rate of 76% for both cortical and white matter lesions with a false positive rate of 29% in comparison to manual segmentation. Finally, it is reported that the proposed methodology achieved to adequately generalize the exams acquired in two hospitals with different scanners.

Gessert *et al* (51) examined a CNN model for lesion segmentation from two time points, using two path architectures. They stratified a cohort of 89 MS patients, with two MRI exams each, baseline and follow-up respectively, while for validation and testing they used a 3-fold cross-validation. Results indicate that the proposed model outperformed classic methodologies, while it was reported a lesion-wise false-positive rate of 26.4% at a true-positive rate of 74.2%.

Essa *et al* (52) proposed an automatic segmentation framework, based on region-based CNN (R-CNN) model applied on T2-w and FLAIR MR images, evaluated on the MICCAI 2008 MS challenge (<http://www.ia.unc.edu/MSseg>). The proposed model shows competitive results compared with the state-of-the-art MS segmentation methods, with average total score 83.25 and average sensitivity 61.8% on the testing set.

Finally, Barquero *et al* (53) developed a CNN architecture (RimNet) for automated rim lesion detection in MS. MR imaging data were acquired from three different scanners, in a cohort of 124 patients. The multimodal RimNet architecture achieved to better classify lesions [area under curve (AUC)=0.943] compared to unimodal approaches, while sensitivity and specificity (70.6 and 94.9%, respectively) were comparable to the experts scores

4. Classification: Diagnosis

During the last years, DL techniques have been successfully applied for the diagnosis and classification of MS disease (54). These techniques can identify patterns of the imaging data without using an explicit feature extraction method, but instead using automatic feature extraction. Advantages stemming from the use of DL techniques in MS diagnosis include the increment of diagnostic accuracy, early stage diagnosis, increase the reliability of the diagnosis, decrease disease related cost, and improvement in patient quality of life. In this section, the most significant research articles in the MS classification using DL techniques are reviewed.

Yoo *et al* (55) presented an automatic framework for detection of MS pathology at an early stage. In this approach, 3D image patches extracted from myelin maps and the corresponding T1-w MR images was used to train a latent joint myelin feature representation using an unsupervised four-layer deep belief network (DBN) framework. This framework used 55 RRMS patients and 44 healthy controls, while by using 11-fold cross validation, it achieved 87.9% average classification accuracy, and authors reported that suggested method was able to identify MS image features from normal appearing brain tissues.

Wang *et al* (56) implemented a 14-layer CNN combined with batch normalization, dropout and stochastic pooling techniques aiming towards early diagnosis and treatment of MS disease. Imaging data for the current study, included 38 MS patients from eHealth laboratory and 26 healthy controls (HC). Results reported that the proposed 14-layer CNN network had sensitivity of 98.77%, specificity 98.76% and accuracy 98.77%, while after comparison of the aforementioned method with maximum pooling, average pooling, five traditional AI methods and a DL method, it was shown that the proposed method outperforms all the above-mentioned techniques.

Zhang *et al* (57) developed a DL algorithm based on CNN that combined parametric rectified linear unit (PReLU) and dropout techniques, in order to accurately separate MS from HC. This study stratified 676 MS brain slices and 681 HC slices, while data augmentation technique was used in order to increase the size of the training set. The 10-layer deep convolutional neural network used in this study was consisted of 7 convolution layers and 3 fully-connected layers. The proposed method achieved 98.22% sensitivity, 98.24% specificity and 98.23% accuracy, while the dropout method increased accuracy by 0.88%, PReLU increased accuracy by 1.92% compared to ordinary ReLU and by 1.48% compared to leaky ReLU.

Talo *et al* (58) implemented a deep transfer learning framework to automatically classify normal and abnormal brain MR images via using a ResNet34 CNN DL model featuring data augmentation, optimal learning rate finder and fine-tuning to adapt a pre-trained model. This study stratified a cohort of 42 subjects (2 HC and 40 patients with cerebrovascular, neoplastic, degenerative, and inflammatory disease types), resulting in 613 images, 27 normal and 513 abnormal, for training and validation. Results from the current study report that they achieved 100% classification accuracy.

Lu *et al* (59) presented a transfer learning technique for automatic detection of pathological brain, by utilizing a pre-trained model featuring AlexNet architecture. In this study brain MR images from 38 HC and 177 pathological were used, including pathologies such as Alzheimer, Glioma, Huntington, AIDS dementia, MS, and Pick. Results reported that the proposed method achieved accuracy of 100% which, outperformed state-of-the-art approaches.

McKinley *et al* (60), investigated the ability of DL algorithm to discriminate radiologically progressive from radiologically stable patients, in 3 different private datasets. To this end, DeepSCAN MS classifier, a fully-convolutional neural network was utilized. The methodology that was used in this study, achieved to temporally track lesion load changes by leveraging measures of uncertainty in the location of lesion boundaries. Results from the present study, disclosed that the proposed framework was able to separate progressive from stable time-points (AUC=0.999) and changes in lesion volume (AUC=0.71). Moreover, method validation on two external datasets confirmed the performance of this method by achieving accuracies 75 and 85% in separating stable and progressive time-points.

Marzullo *et al* (61) introduced a graph convolutional neural network (GCNN) to classify MS patients on four clinical profiles, (CIS, RR, secondary-progressive SP, primary-progressive PP). Methodology in the present study used structural connectivity

information by DWI and evaluated the classification performance using unweighted and weighted connectivity matrices. Moreover, the role of graph-based features aiming to better characterization and classification of the MS pathology were investigated. For the purposes of this study, 90 MS patients (12 CIS, 30 RRMS, 28 SPMS and 20 PPMS) and 24 healthy controls were included in the analysis. Results demonstrated that the aforementioned NN framework offers very good performance in clinical profiles classification, while graph weights representation of brain connections offer significant information for clinical profiles discrimination.

Eitel *et al* (62) presented a DL framework based on a 3D CNN and a layer-wise relevance propagation (LRP) in order to accurately diagnose MS disease. In this study, LRP was used as an additional tool aiming to reveal further relevant image features that will be afterwards forwarded to the trained CNN. The CNN model was trained using MRI data from the Alzheimer Disease Neuroimaging Initiative (921 patients) and afterwards the CNN was used to discriminate among MS (76 patients) and controls (71 healthy controls). Authors reported that the presented methodology showed accuracy 87% and AUC 96%, concluding that LRP in conjunction with proposed CNN is a framework capable of sufficiently classify MS patients and healthy controls.

Narayana *et al* (63) used a CNN in order to evaluate the performance in predicting enhanced MR lesions without using contrast agents. To this end, a CNN was used for classifying lesions from MR images as enhanced or unenhanced. In this study, 1,008 MS patients were involved, while at least one enhancing lesion was observed for 519 participants. MR demyelinating lesions were classified in two classes, enhanced and unenhanced, while performance was assessed by using fivefold cross-validation. Results report sensitivity 78%, specificity 73%, AUC 0.82 for slice-wise prediction, while for participant-wise these were 72%, 70% and 0.75, respectively.

Maggi *et al* (64) proposed a DL based prototype for automated assessment of the central vein sign (CVS) in WM MS lesions. This study included 80 subjects from three different sites, 42 MS, 33 MS mimics with diseases that are described by WM abnormalities similar to MS, and 5 patients with uncertain diagnosis. To this end, a 3D CNN ('CVSnet') was designed, trained on 47 examinations and tested on the remaining 33. Authors reported that the proposed framework achieved human expert performance, achieving lesion-wise median balanced accuracy of 81% and subject-wise balanced accuracy of 89% on the validation and 91% on the test set, while evaluation on data from different hospitals-scanners is promising for larger multi-center trials using the CVS marker in the MS diagnostic criteria.

Wang *et al* (65), utilized a CNN framework in order to discriminate neuromyelitis optical spectrum disorder (NMOSD) (41 patients) from MS (47 patients), a challenging classification problem considering that NMOSD is a rare disease thus there is a limitation in the availability of exams, as well as the lesions in the above mentioned diseases are scattered and overlapping, adding an extra embodiment in the classification procedure. Study results reported that the novel proposed CNN model achieved to better discriminate NMOSD from MS compared to conventional CNN models. More specifically, the proposed method exhibited accuracy 0.75,

sensitivity 0.707, and specificity 0.759, while traditional 3D CNNs that tested on the same problem did not achieve to distinguish the different classes.

Roca *et al* (66) used a DL network in order to predict the expanded disability status scale (EDSS) in a cohort of 1,446 MS patients, partitioned in 971 subjects for training, and 475 subjects for testing. The proposed framework consisted of a CNN model and a classical ML predictor. They finally reported that the proposed method was able to predict two-year EDSS score, based on FLAIR MRI imaging data, while the more informative variables were age, volume of lateral ventricles and the lesion load in main white matter tracts.

Lopatina *et al* (67) utilized a CNN model aiming to identify MS patients by analyzing susceptibility weighted images, considering that in this protocol vein patterns are identifiable and it is also able to indicate extensive demyelination and iron accumulation. The stratified cohort was composed by 66 MS patients and 66 healthy controls, while results indicate that veins located in the anterior medial and lower peripheral regions, are most relevant for the classification decision.

5. Post processing techniques and image enhancement methods

Reducing rescans and recalls is of great importance for the optimization of health care management, since low image quality MR acquisitions often need to be repeated, thus leading to increased hospital costs and extended MR examination times. Furthermore, visual inspection of the related examinations aiming to assess image quality, is impractical in large multi-center studies as well as prone to errors emanating from intra-observer variability. In recent years, computational tools that assess the image quality of the examinations have been developed based on automated assessment of image quality metrics. To this purpose, computer algorithms have been implemented during the last years, aiming to automatically assess image quality as well as acquisition parameters. In this section, recent studies focusing on solving the aforementioned problems by using DL techniques in MR imaging of neurodegenerative diseases are reviewed.

Sreekumari *et al* (68) developed an automated method for assessing the need of rescan, in motion corrupted brain scans. Authors developed a CNN with 7 convolutional layers, 4 max pooling layers, and 3 batch normalization layers that computed the probability for a MR series to be clinically useful, while by combining this probability with a scan dependent and radiologist defined threshold, they determined whether a series need to be rescanned. Moreover, the classification performance was compared with that of 4 technologists and 5 radiologists in 49 series, stemming from MS and stroke patients, characterized by low and moderate motion artefacts. Results indicated that radiologists - technologists produced mean ratio of rescans/recalls of (4.7_5.1)/(9.5_6.8) for MS and (8.6_7.7)/(1.6_1.9) for stroke, while DL produced (7.3_2.2)/(3.2_2.5) for MS, and (3.6_1.5)/(2.8_1.6) for stroke, concluding that this technology independent method can reliably decrease rescan and recall rates.

Sujit *et al* (69) developed a DCNN aiming to automatically evaluate the quality of multicenter structural brain MRI images, using 1,064 images from autism patients from ABIDE

database (60% training, 20% validation and 20% test) while they tested on a cohort of 110 MS patients from the CombiRx dataset (70). The results demonstrated the high accuracy of the proposed method to evaluate image quality of structural brain MRI in multi-center studies (ABIDE dataset achieved AUC 0.90, sensitivity 0.77, specificity 0.85, accuracy 0.84, PPV 0.42, and NPV 0.96 while for the CombiRx there were AUC 0.71, sensitivity 0.41, specificity 0.84, accuracy 0.73, PPV 0.48, and NPV 0.80).

In many applications, the compromise between spatial resolution, SNR, as well as temporal resolution in specific protocols, is limiting the clinical and research applicability of the MR modality. An ordinary approach to overcome this problem is to acquire images with adequate in-plane resolution and low through-plane resolution and afterwards interpolate data, by using super-resolution techniques, in order to obtain isotropic voxels. To this purpose, Zhao *et al* (71) developed a DL method, called SMORE, that accomplished both anti-aliasing and super-resolution using no external atlases. Authors demonstrated the performance of the proposed algorithm in four applications: i) improve visualization of the brain WM lesions in MS patients; ii) improve the visualization of scarring in cardiac left ventricular remodeling after myocardial infarction; iii) performance on multi-view images of the tongue; and iv) improve performance in brain ventricular system parcellation. Regarding the MRI visualization of MS lesions, that is speculated in the present review article, authors examined whether the SMORE computationally enhanced FLAIR images can provide additional diagnostic information compared to a conventional interpolation. For this purpose, FLAIR data was reconstructed from initial resolution of 0.828 x 0.828 mm x 4.4 mm onto a 0.828 x 0.828 mm x 0.828 mm digital grid by a conventional b-spline interpolation, the JogSSR approach that is a super resolution method which improves resolution in the through-plane direction (72), as well as the proposed SMORE algorithm. Authors reported that both JogSSR and SMORE resulted in sharper edges compared to the conventional b-splines interpolation, while SMORE results appeared to be more realistic, however results in this part of the study were assessed only by visual inspection while authors do not provide any quantitative measurement.

Another aspect that has recently gained interest, is the generation of synthetic MR images by using computational techniques. This is an interesting and emerging area of research especially considering that some protocols may be time-consuming and some sequences may be missed due to limited scanning time or patients' interruptions in case of anxiety and confusion. Also, the ability to synthesize information related to different imaging modalities directly from MRI has gained the attention of many researchers in the field of DL in medical imaging.

To this purpose, Wei *et al* (73) used a 3D FCNN to predict FLAIR pulse sequence from other MRI protocols. For this study, 20 MS patients and 4 healthy controls were involved, including T1-w, T2-w, PD, FLAIR, T1 SE and double inversion echo sequences. The performance of the proposed method was compared qualitatively and quantitatively with four state-of-the-art approaches: modality propagation (74), random forests including 60 trees (75), U-Net (76) and voxel

wise multilayer perceptron consisted of two hidden layers and 100 hidden neurons for every layer. Results from this study indicated that the proposed FLAIR synthesis method provides competitive performance to previous techniques. In more detail, the proposed technique was statistically significantly better than the other methods ($P < 0.05$) in average, by providing MSE (SD) 918.07 (41.70) and SSIM(SD) 0.860 (0.031). Finally, authors compared the aforementioned methods in a MS lesion detection task, by evaluating the MS lesion to NAWM as well as to the surrounding NAWM tissue contrast. Also, in this task the proposed method outperformed the competitive techniques on both ratios, revealing that it provides better contrast for MS lesions.

Salem *et al* (77) proposed a synthesis method for MS lesions on MR images aiming to improve the performance of supervised machine learning algorithms, thus avoiding the lack of ground truth. To this end, they used a two-input two-output FCNN for MS lesion synthesis, in which the lesion information was encoded as discrete binary intensities level masks. For this purpose, authors assessed the proposed methodology in two cohorts of patients, by evaluating the similarities among real and synthetic images, as well as by measuring the performance of lesion detection by segmenting both the original and the synthetic images. The two cohorts used included 15 HC and 65 patients with CIS or RRMS, and the ISBI2015 dataset (24) comprising 5 training and 14 testing subjects with 4 to 5 follow-up studies for every subject, while they also used data augmentation techniques. The effect of data augmentation was demonstrated in both analyzed datasets, while results showed the effectiveness of using synthetic MS lesions. Finally, regarding the ISBI2015 challenge, the model was trained using a single image and the synthetic data augmentation and performed similarly to other CNN methods that were fully trained.

Wei *et al* (78) proposed a method to predict positron emission tomography (PET)-derived myelin content map from multimodal MR imaging data, by introducing a new approach called Sketcher-refiner GANs with a specially designed adversarial loss function, in which the Sketcher network generated global anatomical and physiological information, while the Refiner model refined and generated the tissue myelin content. For this purpose, a dataset including 18 MS patients and 10 HC was used, while both MR and PET images were available. It was reported that regarding image quality and myelin content, the proposed approach outperformed the state-of-the-art methods, as well as that prediction results were comparable to PET derived gold standard both in global and voxel-wise levels.

Finck *et al* (79) implemented a diamond shape topology generative adversarial NN (DiamondGAN) in order to produce synthetic double inversion recovery (synthDIR) images while the diagnostic performance of the proposed images was compared to conventional MR images. This study recruited 100 MS patients, while the DiamondGAN was trained in a subset of 50 MS patients and an additional 50 images of generated synthetic data. Results indicate that synthetically generated DIR images resulted in improved detection of juxtacortical lesions, leading to improvement on lesion detection.

Finally, the last category is related to computational methods that are focusing on post-processing MR images

for image reconstruction, and computational analysis. These methods are of great interest considering that they can bypass unreliable computational methods and ill-conditioned mathematical problems, as well as combine large-scale information from multi-site studies by providing quantitatively and qualitatively consistent images to automated algorithms.

Yoon *et al* (80) presented a DL network (QSMnet) with a modified U-net structure able to generate high quality susceptibility source map from single orientation data. A total of 12 healthy controls were used for training, using COSMOS QSM maps, while for evaluation data from a microbleed, a MS and a patient with intraparenchymal hemorrhage were used. Results demonstrated that QSMnet provided superior image quality results compared to TKD and MEDI, while the image quality is comparable to COSMOS.

Bollman *et al* (81) trained a FCNN, DeepQSM, in order to invert the magnetic dipole kernel convolution, and to provide a QSM framework that determines the composition of myelin sheaths of nerve fibers in the brain, as well as to assess quantitative information on iron homeostasis and its dysregulation. This network was trained on synthetic examples, while for testing procedure there were performed four experiments with synthetic data, a single orientation background field corrected tissue phase image and an STI susceptibility map, and finally clinical data from a patient with MS. Study results showed that the proposed methodology enabled identification of deep brain structures, not visible in MRI data. Furthermore, study results revealed that the presented methodology provides information for magnetic tissue properties, and finally showed increased sensitivity in identifying WM lesions regarding the MS patient.

Dewey *et al* (82) proposed a contrast harmonization method, DeepHarmony, by using U-Net DL technique in order to provide images with consistent contrast. To this end, 12 subjects (10 MS and 2 HC) were scanned twice within 30 days, and longitudinal data were retrospectively collected from 45 RRMS patients, while both cohorts were based on two different scanning protocols. Results suggested that DeepHarmony harmonized images showed significant improvement, as well as reduced dependency of atrophy calculations when using DeepHarmony method.

Liu *et al* (83) implemented a fast myelin water fraction (MWF) maps data analysis method, that was based on Myelin Water Imaging data acquired by a 32-echo 3D gradient and spin echo sequence. For this purpose, an NN model was used on data stemming from 4 healthy controls, while for testing there were utilized 1 MS brain, 1 healthy spinal cord, and 2 healthy brains acquired from a different scanner. Results proposed that time for calculation of MWF maps was dramatically reduced while their quality was similar to ground truth levels.

6. Discussion

This review paper aims to shed light on DL applications related to MR imaging in MS and CIS. For this purpose, an extensive search led to 45 original research papers focused on this subject, that were further grouped in three categories i.e. segmentation, classification and a broader category related to image optimization and post processing techniques in MS and CIS. Findings of the current review indicate that there is

Table I. Summary and performance metrics of the reviewed publications relevant to detection-segmentation tasks.

Author (Ref.)	Year	Performance	Architecture	Dataset, #patients (training/test)
Valverde <i>et al</i> (22)	2017	Competition score 87.12 Volume difference down to 40.8 TPR up to 68.7	A cascade of two 3D patch-wise CNNs	45 patients with MS from MICCAI 2008 dataset, and two private MS clinical datasets
Birendaum <i>et al</i> (23)	2017	Dice similarity coefficient 0.627	CNNs based on the single view CNN (V-Net) and the longitudinal network (L-Net)	2015 Longitudinal Multiple Sclerosis Segmentation Challenge
Gros <i>et al</i> (25)	2019	DSC up-to 0.604	A sequence of two CNNs	1,042 subjects; 459 HC, 471 MS, 112 with other spinal pathologies
Aslani <i>et al</i> (28)	2019	DSC up-to 0.611 (ISBI) DSC up-to 0.6655 (private)	Deep end-to-end 2D CNN	37 MS private dataset, and 14 patients with MS from ISBI 2015 longitudinal MS lesion segmentation challenge dataset
Sander <i>et al</i> (29)	2019	Mean % change/SD test-retest 0.45%/0.005 (brainstem) Dice score/SD 0.97/0.005 for brainstem, 0.95/0.0131 for mesencephalon, 0.98/0.006 for pons, 0.95/0.015 for medulla oblongata	MD-GRU	50 patients with MS and 17 HC, 20 independent patients with MS, 50 patients with Alzheimer's
Hashemi <i>et al</i> (31)	2019	DSC 0.703	3D FCNN (FC-DenseNet)	15 patients from the MSSEG of the 2016 Medical Image Computing and Computer Assisted Intervention conference, five patient data from the longitudinal MS lesion segmentation challenge of ISBI conference
Gabr <i>et al</i> (34)	2019	T2 lesion 0.82	FCNN	1,000 patients with RRMS from the CombiRx clinical trial
Weeda <i>et al</i> (35)	2019	SN up-to 0.698	DL CNN method nicMSLesions	14 patients with MS
McKinley <i>et al</i> (40)	2019	DSC 0.58	A cascade of two convolutional neural networks CNNs	122 MRI exams from patients with RRMS (90 patients for training and validation of the classifier, 32 patients for testing), while a second dataset including 10 MRI datasets was used for direct comparison with other centers
Narayana <i>et al</i> (41)	2020	DSC up-to 0.86	FCNN	1,008 patients with clinically definite MS
Nair <i>et al</i> (42)	2020	TPR 0.8, FDR 0.2	3D CNN WITH dropout	1,064 patients with RRMS
McKinley <i>et al</i> (43)	2020	DSC 0.661	Two state-of-the-art CNNs architectures, a 3D Unet consisting of a reference implementation and a more recently proposed architecture, the DeepSCAN	2016 MSSEG training dataset, retrained on a larger dataset comprising of 122 patients with MS (50 training, 40 validation and 32 patients for testing)
Narayana <i>et al</i> (44)	2020	DSC up-to 0.91 (FLAIR) DSC up-to 0.90 (FLAIR, PD, T1, T2) DSC up-to 0.60 (PD)	U-net, a fully CNN	1,000 patients with MS

Table I. Continued.

Author (Ref.)	Year	Performance	Architecture	Dataset, #patients (training/test)
Salem <i>et al</i> (45)	2020	DSC for detection 0.83, DSC for segmentation 0.55	FCNN	60 early patients with MS and CIS
Brown <i>et al</i> (46)	2020	Not applicable.	FCNN similar to U-net	1,018 scans from 256 participants in a study of pediatric-onset MS
Ackaouy <i>et al</i> (47)	2020	No table with absolute measurements, too many combinations of multi-centric experiments, only boxplot results	3D-Unet	53 patients with MS from MICCAI 2016 MS lesion segmentation challenge
Coronado <i>et al</i> (49)	2020	DSC 0.77	3D CNN	1,006 patients with RRMS
La Rosa <i>et al</i> (50)	2020	DSC 0.62	FCNN architecture based on the 3D U-Net	90 patients with MS
Gessert <i>et al</i> (51)	2020	DSC up-to 0.656	CNN	89 patients with MS
Essa <i>et al</i> (52)	2020	VD down to 0.451, TPR 0.681, FPR 0.632	Region-based CNN	45 patients with MS from MICCAI 2008
Barquero <i>et al</i> (53)	2020	DSC 0.835	CNN (RimNet)	124 patients with MS

CNNs, convolution neural networks; MS, multiple sclerosis; MD-GRU, multi-dimensional gated recurrent units; SD, standard deviation; HC, healthy controls; DSC, Dice Similarity Coefficient; ISBI, International Symposium on Biomedical Imaging; TPR, true positive rate; FCNN, fully convolutional neural network; MSSEG, MS lesion segmentation challenge; RRMS, relapsing-remitting multiple sclerosis; SN, sensitivity; MRI, magnetic resonance imaging; FLAIR, fluid-attenuated inversion recovery; PD, proton density; CIS, clinically isolated syndrome; MICCAI, medical image computing and computer assisted intervention society; VD, volume difference.

a growing interest during the last years towards applying DL techniques for segmentation and classification related to MS imaging studies.

A performance analysis was conducted by grouping the studies into three main categories based on imaging tasks such as segmentation in Table I, classification in Table II and various image processing tasks (synthesis, quality assessment, image enhancement, etc) in Table III. A few important issues in comparing these studies namely are: i) the lack of a clear data stratification protocol (57-59); ii) applying ‘good practices’ such as use of separate internal and external validation sets (28); iii) incorporating an adequate number of patients for DL model convergence (35,83); iv) evaluating with appropriate metrics (42,59) like AUC in addition to ACC in binary classification tasks; and v) incorporating different metrics for the same task such as DSC (23) versus VD (22) in segmentation. Thus, reporting the aforementioned performance measurements was a difficult task which included interpreting figures, highly variable experimental settings and, most importantly, identifying metrics on unseen testing sets (if available) versus internal validation sets which were also used in optimizing the models. Nevertheless, Narayana *et al* (44) proposed a FLAIR-based lesion segmentation with a testing DSC of 0.91 and Sander *et al* (29) utilized a multi-dimensional gated recurrent unit model achieving a performance up-to DSC 0.97. In MS classification, McKinley *et al* (60) achieved sensitivity up-to 0.72 on two different external validation sets, similar to Narayana *et al* (63) (SN 0.72) on patient-basis versus SN 0.78 on a slice-basis in the same study.

Concerning the limitations of the reviewed papers, the most pronounced are associated with the absence of ground truth, the small available cohorts, and the lack of generalization of

the results in multi-center data from diverse vendors, in Fig. 4 presents the limitations of the reviewed literature grouped in a chart pie. Finally, another noticeable limitation of DL techniques is the lack of explainability, which is particularly critical for the clinical translation of such methods to clinical practice as well as for adding precision in MS and CIS diagnosis and disease management.

Considering the segmentation procedure, the fundamental MRI protocols, T1-w, T2-w and PD can be characterized based on their advantages concluding that, T1-w images enclose detailed anatomical information and thus facilitate image registration tasks involved in e.g. development of brain atlases. On the contrary, T2-w images are beneficial for highlighting WM lesions which appear as bright areas, thus assisting lesion detection tasks. However, the main drawback of these techniques is the insufficient differentiation of CSF, GM and lesions in terms of image contrast. Finally, PD-w images are beneficial in revealing MS lesions as areas of increased contrast compared to WM, even better than T2-w, but still the relative image contrast between MS lesions and CSF are in the same range of intensities. A major limitation for accurate image segmentation is pixel misclassification due to the partial volume effect generated from the low spatial resolution of the MR protocols which renders difficult the accurate delineation of brain regions and decreases the accuracy of volumetric studies. Finally, inter-observer variability is a major problem when trying to generate ground truth label data, while some of the factors that may hamper this task include image quality, different levels of user expertise and domain knowledge. Concerning the reviewed research studies, in Narayana *et al* (41) segmentation results were assessed by

Table II. Summary and performance metrics of the reviewed publications relevant to classification tasks.

Author (Ref.)	Year	Performance	Architecture	Dataset, #patients (training/test)
Yoo <i>et al</i> (55)	2018	ACC 0.879, SN 0.873, SP 0.886, AUC 0.88	Unsupervised four-layer DBN	55 patients with RRMS and 44 HC
Wang <i>et al</i> (56)	2018	ACC 0.988, SN 0.988, SP 0.988	14-layer CNN combined with batch normalization, dropout and stochastic pooling techniques	38 patients with MS from eHealth laboratory and 26 HC
Zhang <i>et al</i> (57)	2018	ACC 0.982, SN 0.982, SP 0.982	10-layer deep convolutional neural network used in this study was consisted of 7 convolution layers and 3 fully-connected layers	676 MS brain slices and 681 HC slices
Talo <i>et al</i> (58)	2019	Stage-1: ACC 0.979, SN 0.778, Stage-2: ACC 0.979, SN 0.74 Stage-3: ACC 1, SN 1	CNN based ResNet34	42 subjects (2 HC and 40 patients with cerebrovascular, neoplastic, degenerative and inflammatory disease types)
Lu <i>et al</i> (59)	2019	ACC 1	AlexNet structure and stochastic gradient descent with momentum transfer learning technique	MR images from 38 HC and 177 pathological, including pathologies such as Alzheimer's, glioma, Huntington's, AIDS dementia, MS and Pick's
McKinley <i>et al</i> (60)	2019	External validation sets: Zurich: ACC 0.75, SN 0.60 Munich: ACC 0.85, SN 0.72	DeepSCAN MS classifier, a fully-convolutional neural network	Bern (train-test), Zurich and Munich datasets
Marzullo <i>et al</i> (61)	2019	F1 0.74, PR 0.76, RC 0.75	Graph CNN	90 patients with MS (12 CIS, 30 RRMS, 28 SPMS and 20 PPMS) and 24 HC
Eitel <i>et al</i> (62)	2019	ACC 0.87, AUC 0.96	3D CNN and a LRP	921 patients with Alzheimer's disease for training, validation in 76 MS and 71 HC
Narayana <i>et al</i> (63)	2020	Slice: AUC 0.82, SN 0.78, SP 0.73 Patient: AUC 0.75, SN 0.72, SP 0.70	CNN (fully connected)	1,008 participants with MS
Maggi <i>et al</i> (64)	2020	ACC 0.91, SN 0.89, SP 0.92 Vesselness: ACC 0.69, SN 0.61, SP 0.77	3D CNN ('CVSnet')	42 MS, 33 MS mimics and 5 patients with uncertain diagnosis
Wang <i>et al</i> (65)	2020	ACC 0.75, SN 0.707, SP 0.759	CNN	41 patients with NMOSD and 47 patients with MS
Roca <i>et al</i> (66)	2020	MSE 3	CNN	1,446 MS (971 training, 475 testing)
Lopatina <i>et al</i> (67)	2020	ACC up-to 0.95 (echo 1)	CNN	66 MS and 66 healthy controls

SP, secondary progressive; AUC, area under curve; DBN, deep belief network; HC, healthy controls; CNN, convolution neural networks; MS, multiple sclerosis; MR, magnetic resonance; CIS, clinically isolated syndrome; LRP, layer-wise relevance propagation; NMOSD, neuromyelitis optical spectrum disorder; MSE, mean square error; ACC, accuracy; SN, sensitivity; RRMS, relapsing-remitting multiple sclerosis; PR, precision; RC, recall; SPMS, secondary progressive multiple sclerosis; PPMS, primary progressive multiple sclerosis.

two experts, while in the study from Brown *et al* (46) results were evaluated with manual segmentations stemming from only one expert.

Considering the classification related task, initially it can be reported that fundamentally this is not a binary problem. CIS diagnosis adds another level of complexity to the clas-

sification problem, which can be treated as multiple binary comparisons, i.e., controls vs. MS, controls vs. CIS, CIS vs. MS, while for each problem a different classifier can be developed. Furthermore, considering the constantly increasing imaging databases, especially those including longitudinal data, research studies may shift to the development of CAD based

Table III. Summary and performance metrics of the reviewed publications relevant to imaging protocol related tasks.

Sub-category	Author (Ref.)	Year	Performance mean (standard deviation)	Architecture	Dataset, #patients (training/test)
Image quality evaluation	Sreekumari <i>et al</i> (68)	2019	Not applicable	CNN with seven convolutional layers, four max pooling layers and three batch normalization layers DCNN	MS and stroke patients
Image quality evaluation	Sujit <i>et al</i> (69)	2019	ABIDE: AUC 0.90, ACC 0.84, SN 0.77, SP 0.85 CombiRx: AUC 0.71, ACC 0.73, SN 0.41, SP 0.84		1,064 images from patients with autism from ABIDE database (60% training, 20% validation and 20% test), and 110 patients with MS from the CombiRx dataset
Enhance image	Zhao <i>et al</i> (71)	2019	Not applicable	A DL method called SMORE, Enhanced Deep Residual Network 3D FCNN	Brain white matter lesions from patients with MS quality 20 patients with MS and 4 HC
Generate synthetic images	Wei <i>et al</i> (73)	2019	MSE 918.07 (41.70) SSIM 0.860 (0.031)		
Generate synthetic images	Salem <i>et al</i> (77)	2019	T1w: MSE 0.03, SSIM 0.96 FLAIR: MSE 0.02, SSIM 0.98	A two-input two-output FCNN for MS lesion synthesis, in which the lesion information was encoded as discrete binary intensities level masks	15 HC and 65 patients with CIS or RRMS, and the ISBI2015 dataset consisted of five training and 14 testing subjects with four to five follow-up studies for every subject 18 patients with MS and 10 HC
Generate synthetic images	Wei <i>et al</i> (78)	2019	MSE: 0.0083, PSNR 30.044	Sketcher-refiner GANs	
Generate synthetic images	Finck <i>et al</i> (79)	2020	Not applicable	A diamond shape topology generative adversarial NN (DiamondGAN)	110 patients with MS
Computational analysis	Yoon <i>et al</i> (80)	2018	pSNR 42.6 (0.61) NRMSE 54.3 (2.5) HFEN 51.8 (2.5) SSIM 0.90 (0.01)	DL network (QSMnet) with a modified U-net structure	12 HC, a microbleed, a MS and a haemorrhage patient
Computational analysis	Bollman <i>et al</i> (81)	2019	NRMSE 41.29 HFEN 23.69 SDSIM 0.21	FCNN, DeepQSM	Synthetic data, and a clinical dataset from a patient with MS
Computational analysis	Dewey <i>et al</i> (82)	2019	Not applicable	U-Net	10 MS and two HC were scanned twice, longitudinal retrospective data from 45 patients with RRMS
Computational analysis	Liu <i>et al</i> (83)	2020	Myelin water fraction 0.039 (0.037)	NN	MWI data acquired by a 32-echo 3D gradient and spin echo sequence, 6 healthy patients and one MS

ABIDE, Autism Brain Imaging Data Exchange; SP, secondary progressive; NN, neural networks; HFEN, high-frequency error norm; SDSIM, Structural Dissimilarity Index; ACC, accuracy; SN, sensitivity; DCNN, deep convolutional neural networks; SMORE, Synthetic Multi-Orientiation Resolution Enhancement; MSE, mean square error; SSIM, structure similarity index; RRMS, relapsing-remitting multiple sclerosis; GANs, generative adversarial network; pSNR, peak signal-to-noise ratio; NRMSE, normalized root mean-squared error.

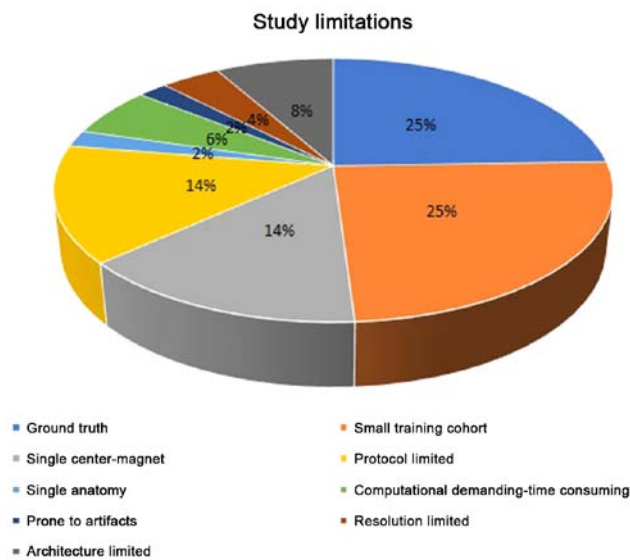


Figure 4. Study limitations of the relevant publications presented in a pie chart. Most common limitations in the reviewed research article were the small training cohort and the lack of ground truth.

systems for early detection of the MS disease. In addition, classification techniques can be grouped in class-based methods in which MS lesions are separated in WM, GM and CSF lesions, and outlier-based methods in which GM, WM, and CSF are distinct classes from MS lesions.

Furthermore, images stemming from different centers, scanners and protocols, provide a basis in order to build robust algorithms that can generalize the aforementioned tasks. However, in the small dataset setting, transfer learning techniques are methods used for alleviating the limited availability of training samples by tuning parameters of pre-trained networks with less data in order to adapt existing models in new domains and achieve higher level of generalization. In domain adaptation techniques, optimal transfer is established through a source and a target domain in order to deploy a model on the target site that was not included in the training process, and this is a promising research field for providing integrated solutions.

Moreover, according to best practices that must be followed in order to build a robust DL methodology, some research studies mentioned in this review article might not satisfy these prerequisites. More specific, Ackaouy *et al* (47) and Talo *et al* (58) methodology did not follow the universally accepted best practices in DL training, considering the data splitting. Data should be split into training set, validation set and testing set in order to ensure that the model will not be over-fitted. External validation set is necessary in order to enhance reproducibility and generalizability of a prediction model to new patients. In the reviewed research articles, only a few used external validation set in order to check reproducibility and enhance generalizability (29,34,40,60,71).

Finally, data imbalance problem is very common in MS machine learning applications and can lead to a training network with sufficient high prediction but low recall, thus biased to the class with the most data. Techniques such as two-step training, sample re-weighting, balance sampling and similarity loss functions are promising for bypassing such

problems, while they can, also, provide computational techniques suited to highly unbalanced problems.

Future DL research work on MS considering also the aforementioned limitations, should focus on three different directions. The first direction regards the formation of large and more diverse datasets, with optimized protocols, for providing a ground truth validation framework of existing and future techniques. The second direction concerns the need for MS imaging data harmonization techniques for reducing the inherent information heterogeneity of multi-centric data due to different vendors and protocols and enabling the development of more robust and accurate AI models. Finally, the development of CAD systems for early detection of MS disease is of great importance based on the increased availability of larger datasets. Such systems offering cloud-based AI services, can provide an enhanced diagnostic experience to clinicians and offer better diagnostic opportunities especially in rural areas that usually lack access to specialists. All these directions regarding the future of DL in MS have to promote explainability and trustworthiness, and not only target increased performance, in order to realize the vision of real-world use of AI algorithms in clinical practice.

Acknowledgements

Not applicable.

Funding

No funding was received.

Availability of data and materials

Not applicable.

Authors' contributions

EEK, EP and KM conceived the designed study. EEK, EP, ET and KM researched the literature, performed analysis and interpretation of data and drafted the manuscript. EEK, EP, ET, TGM, PS, GZP, AT, DAS, AK and KM critically revised the article for important intellectual content. All authors have read and approved the final manuscript. Data sharing is not applicable.

Ethics approval and consent to participate

Not applicable.

Patient consent for publication

Not applicable.

Competing interests

DAS is the Editor-in-Chief of the journal, but had no personal involvement in the reviewing process, or any influence in terms of adjudicating on the final decision for this article. All the authors declare that they have no competing interests.

References

1. Ortiz GG, Pacheco-Moisés FP, Macías-Islas MÁ, Flores-Alvarado LJ, Mireles-Ramírez MA, González-Renovato ED, Hernández-Navarro VE, Sánchez-López AL and Alatorre-Jiménez MA: Role of the blood-brain barrier in multiple sclerosis. *Arch Med Res* 45: 687-697, 2014.
2. Lopes Pinheiro MA, Kooij G, Mizee MR, Kamermans A, Enzmann G, Lyck R, Schwanger M, Engelhardt B and de Vries HE: Immune cell trafficking across the barriers of the central nervous system in multiple sclerosis and stroke. *Biochim Biophys Acta* 1862: 461-471, 2016.
3. Miller DH, Chard DT and Ciccarelli O: Clinically isolated syndromes. *Lancet Neurol* 11: 157-169, 2012.
4. Kappos L, Polman CH, Freedman MS, Edan G, Hartung HP, Miller DH, Montalban X, Barkhof F, Bauer L, Jakobs P, *et al*: Treatment with interferon beta-1b delays conversion to clinically definite and McDonald MS in patients with clinically isolated syndromes. *Neurology* 67: 1242-1249, 2006.
5. Fu Y, Talavage TM and Cheng JX: New imaging techniques in the diagnosis of multiple sclerosis. *Expert Opin Med Diagn* 2: 1055-1065, 2008.
6. Horsfield MA, Rovaris M, Rocca MA, Rossi P, Benedict RH, Filippi M and Bakshi R: Whole-brain atrophy in multiple sclerosis measured by two segmentation processes from various MRI sequences. *J Neurol Sci* 216: 169-177, 2003.
7. van Walderveen MA, Kamphorst W, Scheltens P, van Waesberghe JH, Ravid R, Valk J, Polman CH and Barkhof F: Histopathologic correlate of hypointense lesions on T1-weighted spin-echo MRI in multiple sclerosis. *Neurology* 50: 1282-1288, 1998.
8. Bakshi R, Ariyaratana S, Benedict RH and Jacobs L: Fluid-attenuated inversion recovery magnetic resonance imaging detects cortical and juxtacortical multiple sclerosis lesions. *Arch Neurol* 58: 742-748, 2001.
9. Polman CH, Reingold SC, Edan G, Filippi M, Hartung HP, Kappos L, Lublin FD, Metz LM, McFarland HF, O'Connor PW, *et al*: Diagnostic criteria for multiple sclerosis: 2005 revisions to the 'McDonald Criteria'. *Ann Neurol* 58: 840-846, 2005.
10. Richards TL: Proton MR spectroscopy in multiple sclerosis: Value in establishing diagnosis, monitoring progression, and evaluating therapy. *AJR Am J Roentgenol* 157: 1073-1078, 1991.
11. Pike GB, De Stefano N, Narayanan S, Worsley KJ, Pelletier D, Francis GS, Antel JP and Arnold DL: Multiple sclerosis: Magnetization transfer MR imaging of white matter before lesion appearance on T2-weighted images. *Radiology* 215: 824-830, 2000.
12. Filippi M and Rocca MA: Magnetization transfer magnetic resonance imaging in the assessment of neurological diseases. *J Neuroimaging* 14: 303-313, 2004.
13. Rovaris M, Gass A, Bammer R, Hickman SJ, Ciccarelli O, Miller DH and Filippi M: Diffusion MRI in multiple sclerosis. *Neurology* 65: 1526-1532, 2005.
14. Lapointe E, Li DKB, Trabulsee AL and Rauscher A: What Have We Learned from Perfusion MRI in Multiple Sclerosis? *AJNR Am J Neuroradiol* 39: 994-1000, 2018.
15. Kotsiantis SB, Zaharakis I and Pintelas P: Supervised machine learning: A review of classification techniques. *Emerging artificial intelligence applications in computer engineering* 160: 3-24, 2007.
16. Mortazavi D, Kouzani AZ and Soltanian-Zadeh H: Segmentation of multiple sclerosis lesions in MR images: A review. *Neuroradiology* 54: 299-320, 2012.
17. Uddin M, Wang Y and Woodbury-Smith M: Artificial intelligence for precision medicine in neurodevelopmental disorders. *NPJ Digit Med* 2: 112, 2019.
18. Bergsland N, Horakova D, Dwyer MG, Uher T, Vaneckova M, Tyblova M, Seidl Z, Krasensky J, Havrdova E and Zivadinov R: Gray matter atrophy patterns in multiple sclerosis: A 10-year source-based morphometry study. *Neuroimage Clin* 17: 444-451, 2017.
19. Pontillo G, Petracca M, Coccozza S and Brunetti A: The Development of Subcortical Gray Matter Atrophy in Multiple Sclerosis: One Size Does Not Fit All. *AJNR Am J Neuroradiol* 41: E80-E81, 2020.
20. Almutairi AH, Hassan HA, Suppiah S, Alomair OI, Alshoabi A, Almutairi H and Mahmud R: Lesion load assessment among multiple sclerosis patient using DIR, FLAIR, and T2WI sequences. *Egypt J Radiol Nucl Med* 51: 209, 2020.
21. Thompson AJ, Banwell BL, Barkhof F, Carroll WM, Coetzee T, Comi G, Correale J, Fazekas F, Filippi M, Freedman MS, *et al*: Diagnosis of multiple sclerosis: 2017 revisions of the McDonald criteria. *Lancet Neurol* 17: 162-173, 2018.
22. Valverde S, Cabezas M, Roura E, González-Villà S, Pareto D, Vilanova JC, Ramió-Torrentà L, Rovira À, Oliver A and Lladó X: Improving automated multiple sclerosis lesion segmentation with a cascaded 3D convolutional neural network approach. *Neuroimage* 155: 159-168, 2017.
23. Birenbaum A and Greenspan H: Multi-view longitudinal CNN for multiple sclerosis lesion segmentation. *Eng Appl Artif Intell* 65: 111-118, 2017.
24. Carass A, Roy S, Jog A, Cuzzocreo JL, Magrath E, Gherman A, Button J, Nguyen J, Bazin PL, Calabresi PA, *et al*: Longitudinal multiple sclerosis lesion segmentation data resource. *Data Brief* 12: 346-350, 2017.
25. Gros C, De Leener B, Badji A, Maranzano J, Eden D, Dupont SM, Talbott J, Zhuoquiong R, Liu Y, Granberg T, *et al*: Automatic segmentation of the spinal cord and intramedullary multiple sclerosis lesions with convolutional neural networks. *Neuroimage* 184: 901-915, 2019.
26. Milletari F, Navab N and Ahmadi SA: V-Net: Fully Convolutional Neural Networks for Volumetric Medical Image Segmentation. In: *Proceedings of the 2016 Fourth International Conference on 3D Vision (3DV)*. IEEE, Stanford, CA, pp565-571, 2016.
27. De Leener B, Kadoury S and Cohen-Adad J: Robust, accurate and fast automatic segmentation of the spinal cord. *Neuroimage* 98: 528-536, 2014.
28. Aslani S, Dayan M, Storelli L, Filippi M, Murino V, Rocca MA and Sona D: Multi-branch convolutional neural network for multiple sclerosis lesion segmentation. *Neuroimage* 196: 1-15, 2019.
29. Sander L, Pezold S, Andermatt S, Amann M, Meier D, Wendebourg MJ, Sinnecker T, Radue EW, Naegelin Y, Granziera C, *et al*: Alzheimer's Disease Neuroimaging Initiative: Accurate, rapid and reliable, fully automated MRI brainstem segmentation for application in multiple sclerosis and neurodegenerative diseases. *Hum Brain Mapp* 40: 4091-4104, 2019.
30. Iglesias JE, Van Leemput K, Bhatt P, Casillas C, Dutt S, Schuff N, Truran-Sacrey D, Boxer A and Fischl B: Alzheimer's Disease Neuroimaging Initiative: Bayesian segmentation of brainstem structures in MRI. *Neuroimage* 113: 184-195, 2015.
31. Hashemi SR, Salehi SSM, Erdogmus D, Prabhu SP, Warfield SK and Gholipour A: Asymmetric Loss Functions and Deep Densely Connected Networks for Highly Imbalanced Medical Image Segmentation: Application to Multiple Sclerosis Lesion Detection. *IEEE Access* 7: 721-1735, 2019.
32. Commowick O, Cervenansky F and Ameli R: MSSEG challenge proceedings: multiple sclerosis lesions segmentation challenge using a data management and processing infrastructure. MICCAI, Athens, 2016.
33. Carass A, Roy S, Jog A, Cuzzocreo JL, Magrath E, Gherman A, Button J, Nguyen J, Prados F, Sudre CH, *et al*: Longitudinal multiple sclerosis lesion segmentation: Resource and challenge. *Neuroimage* 148: 77-102, 2017.
34. Gabr RE, Coronado I, Robinson M, Sujit SJ, Datta S, Sun X, Allen WJ, Lublin FD, Wolinsky JS and Narayana PA: Brain and lesion segmentation in multiple sclerosis using fully convolutional neural networks: A large-scale study. *Mult Scler* 26: 1217-1226, 2020.
35. Weeda MM, Brouwer I, de Vos ML, de Vries MS, Barkhof F, Pouwels PJW and Vrenken H: Comparing lesion segmentation methods in multiple sclerosis: Input from one manually delineated subject is sufficient for accurate lesion segmentation. *Neuroimage Clin* 24: 102074, 2019.
36. Valverde S, Salem M, Cabezas M, Pareto D, Vilanova JC, Ramió-Torrentà L, Rovira À, Salvi J, Oliver A and Lladó X: One-shot domain adaptation in multiple sclerosis lesion segmentation using convolutional neural networks. *Neuroimage Clin* 21: 101638, 2019.
37. Shiee N, Bazin PL, Ozturk A, Reich DS, Calabresi PA and Pham DL: A topology-preserving approach to the segmentation of brain images with multiple sclerosis lesions. *Neuroimage* 49: 1524-1535, 2010.
38. Schmidt P: Bayesian Inference for Structured Additive Regression Models for Large-Scale Problems with Applications to Medical Imaging (unpublished PhD thesis). Ludwig-Maximilians-Universität München, 2016.

39. Griffanti L, Zamboni G, Khan A, Li L, Bonifacio G, Sundaresan V, Schulz UG, Kuker W, Battaglini M, Rothwell PM, *et al*: BIANCA (Brain Intensity AbNormality Classification Algorithm): A new tool for automated segmentation of white matter hyperintensities. *Neuroimage* 141: 191-205, 2016.
40. McKinley R, Wepfer R, Aschwanden F, Grunder L, Muri R, Rummel C, Verma R, Weisstanner C, Reyes M, Salmen A, *et al*: Simultaneous lesion and neuroanatomy segmentation in multiple sclerosis using deep neural networks. arXiv:1901.07419.
41. Narayana PA, Coronado I, Sujit SJ, Wolinsky JS, Lublin FD and Gabr RE: Deep-Learning-Based Neural Tissue Segmentation of MRI in Multiple Sclerosis: Effect of Training Set Size. *J Magn Reson Imaging* 51: 1487-1496, 2020.
42. Nair T, Precup D, Arnold DL and Arbel T: Exploring uncertainty measures in deep networks for Multiple sclerosis lesion detection and segmentation. *Med Image Anal* 59: 101557, 2020.
43. McKinley R, Wepfer R, Aschwanden F, Grunder L, Muri R, Rummel C, Verma R, Weisstanner C, Reyes M, Salmen A, *et al*: Simultaneous lesion and brain segmentation in multiple sclerosis using deep neural networks. *Sci Rep* 11: 1087, 2021.
44. Narayana PA, Coronado I, Sujit SJ, Sun X, Wolinsky JS and Gabr RE: Are multi-contrast magnetic resonance images necessary for segmenting multiple sclerosis brains? A large cohort study based on deep learning. *Magn Reson Imaging* 65: 8-14, 2020.
45. Salem M, Valverde S, Cabezas M, Pareto D, Oliver A, Salvi J, Rovira À and Lladó X: A fully convolutional neural network for new T2-w lesion detection in multiple sclerosis. *Neuroimage Clin* 25: 102149, 2020.
46. Brown RA, Fetco D, Fratila R, Fadda G, Jiang S, Alkhawajah NM, Yeh EA, Banwell B, Bar-Or A and Arnold DL; Canadian Pediatric Demyelinating Disease Network: Deep learning segmentation of orbital fat to calibrate conventional MRI for longitudinal studies. *Neuroimage* 208: 116442, 2020.
47. Ackaouy A, Courty N, Vallée E, Commowick O, Barillot C and Galassi F: Unsupervised Domain Adaptation With Optimal Transport in Multi-Site Segmentation of Multiple Sclerosis Lesions From MRI Data. *Front Comput Neurosci* 14: 19, 2020.
48. Commowick O, Istace A, Kain M, Laurent B, Leray F, Simon M, Pop SC, Girard P, Améli R, Ferré JC, *et al*: Objective Evaluation of Multiple Sclerosis Lesion Segmentation using a Data Management and Processing Infrastructure. *Sci Rep* 8: 13650, 2018.
49. Coronado I, Gabr RE and Narayana PA: Deep learning segmentation of gadolinium-enhancing lesions in multiple sclerosis. *Mult Scler* 27: 219-527, 2021.
50. La Rosa F, Abdulkadir A, Fartaria MJ, Rahmzadeh R, Lu PJ, Galbusera R, Barakovic M, Thiran JP, Granziera C and Cuadra MB: Multiple sclerosis cortical and WM lesion segmentation at 3T MRI: A deep learning method based on FLAIR and MP2RAGE. *Neuroimage Clin* 27: 102335, 2020.
51. Gessert N, Krüger J, Opfer R, Ostwaldt AC, Manogaran P, Kitzler HH, Schippling S and Schlaefler A: Multiple sclerosis lesion activity segmentation with attention-guided two-path CNNs. *Comput Med Imaging Graph* 84: 101772, 2020.
52. Essa E, Aldesouky D, Hussein SE and Rashad MZ: Neuro-fuzzy patch-wise R-CNN for multiple sclerosis segmentation. *Med Biol Eng Comput* 58: 2161-2175, 2020.
53. Barquero G, La Rosa F, Kebiri H, Lu PJ, Rahmzadeh R, Weigel M, Fartaria MJ, Kober T, Théaudin M, Du Pasquier R, *et al*: RimNet: A deep 3D multimodal MRI architecture for paramagnetic rim lesion assessment in multiple sclerosis. *Neuroimage Clin* 28: 102412, 2020.
54. Gautam R and Sharma M: Prevalence and Diagnosis of Neurological Disorders Using Different Deep Learning Techniques: A Meta-Analysis. *J Med Syst* 44: 49, 2020.
55. Yoo Y, Tang LYW, Brosch T, Li DKB, Kolind S, Vavasour I, Rauscher A, MacKay AL, Traboulsee A and Tam RC: Deep learning of joint myelin and T1w MRI features in normal-appearing brain tissue to distinguish between multiple sclerosis patients and healthy controls. *Neuroimage Clin* 17: 169-178, 2017.
56. Wang SH, Tang C, Sun J, Yang J, Huang C, Phillips P and Zhang YD: Multiple Sclerosis Identification by 14-Layer Convolutional Neural Network With Batch Normalization, Dropout, and Stochastic Pooling. *Front Neurosci* 12: 818, 2018.
57. Zhang YD, Pan C, Sun J and Tang C: Multiple sclerosis identification by convolutional neural network with dropout and parametric ReLU. *J Comput Sci* 28: 818, 2018.
58. Talo M, Baloglu UB, Yıldırım Ö and Acharya UR: Application of deep transfer learning for automated brain abnormality classification using MR images. *Cogn Syst Res* 54: 176-188, 2019.
59. Lu S, Lu Z and Zhang YD: Pathological brain detection based on AlexNet and transfer learning. *J Comput Sci* 30: 41-47, 2019.
60. McKinley R, Wepfer R, Grunder L, Aschwanden F, Fischer T, Friedli C, Muri R, Rummel C, Verma R, Weisstanner C, *et al*: Automatic detection of lesion load change in Multiple Sclerosis using convolutional neural networks with segmentation confidence. *Neuroimage Clin* 25: 102104, 2020.
61. Marzullo A, Kocevar G, Stamile C, Durand-Dubief F, Terracina G, Calimeri F and Sappey-Marinié D: Classification of Multiple Sclerosis Clinical Profiles via Graph Convolutional Neural Networks. *Front Neurosci* 13: 594, 2019.
62. Eitel F, Soehler E, Bellmann-Strobl J, Brandt AU, Ruprecht K, Giess RM, Kuchling J, Asseger S, Weygandt M, Haynes JD, *et al*: Uncovering convolutional neural network decisions for diagnosing multiple sclerosis on conventional MRI using layer-wise relevance propagation. *Neuroimage Clin* 24: 102003, 2019.
63. Narayana PA, Coronado I, Sujit SJ, Wolinsky JS, Lublin FD and Gabr RE: Deep Learning for Predicting Enhancing Lesions in Multiple Sclerosis from Noncontrast MRI. *Radiology* 294: 398-404, 2020.
64. Maggi P, Fartaria MJ, Jorge J, La Rosa F, Absinta M, Sati P, Meuli R, Du Pasquier R, Reich DS, Cuadra MB, *et al*: CVSnet: A machine learning approach for automated central vein sign assessment in multiple sclerosis. *NMR Biomed* 33: e4283, 2020.
65. Wang Z, Yu Z, Wang Y, Zhang H, Luo Y, Shi L, Wang Y and Guo C: 3D Compressed Convolutional Neural Network Differentiates Neuromyelitis Optical Spectrum Disorders From Multiple Sclerosis Using Automated White Matter Hyperintensities Segmentations. *Front Physiol* 11: 612928, 2020.
66. Roca P, Attye A, Colas L, Tucholka A, Rubini P, Cackowski S, Ding J, Budzik JF, Renard F, Doyle S, *et al*: OFSEP Investigators; Steering Committee; Investigators; Imaging group: Artificial intelligence to predict clinical disability in patients with multiple sclerosis using FLAIR MRI. *Diagn Interv Imaging* 101: 795-802, 2020.
67. Lopatina A, Ropele S, Sibgatulin R, Reichenbach JR and Güllmar D: Investigation of Deep-Learning-Driven Identification of Multiple Sclerosis Patients Based on Susceptibility-Weighted Images Using Relevance Analysis. *Front Neurosci* 14: 609468, 2020.
68. Sreekumari A, Shanbhag D, Yeo D, Foo T, Pilitsis J, Polzin J, Patil U, Coblentz A, Kapadia A, Khinda J, *et al*: A Deep Learning-Based Approach to Reduce Rescan and Recall Rates in Clinical MRI Examinations. *AJNR Am J Neuroradiol* 40: 217-223, 2019.
69. Sujit SJ, Coronado I, Kamali A, Narayana PA and Gabr RE: Automated image quality evaluation of structural brain MRI using an ensemble of deep learning networks. *J Magn Reson Imaging* 50: 1260-1267, 2019.
70. Lublin FD, Cofield SS, Cutter GR, Conwit R, Narayana PA, Nelson F, Salter AR, Gustafson T and Wolinsky JS; CombiRx Investigators: Randomized study combining interferon and glatiramer acetate in multiple sclerosis. *Ann Neurol* 73: 327-340, 2013.
71. Zhao C, Shao M, Carass A, Li H, Dewey BE, Ellingsen LM, Woo J, Guttman MA, Blitz AM, Stone M, *et al*: Applications of a deep learning method for anti-aliasing and super-resolution in MRI. *Magn Reson Imaging* 64: 132-141, 2019.
72. Jog A, Carass A and Prince JL: Self Super-resolution for Magnetic Resonance Images. *Med Image Comput Comput Assist Interv* 9902: 553-560, 2016.
73. Wei W, Poirion E, Bodini B, Durrleman S, Colliot O, Stankoff B and Ayache N: Fluid-attenuated inversion recovery MRI synthesis from multisequence MRI using three-dimensional fully convolutional networks for multiple sclerosis. *J Med Imaging (Bellingham)* 6: 014005, 2019.
74. Ye DH, Zikic D, Glocker B, Criminisi A and Konukoglu E: Modality propagation: coherent synthesis of subject-specific scans with data-driven regularization. *Med Image Comput Comput Assist Interv* 13: 606-613, 2013.
75. Jog A, Carass A, Pham DL and Prince JL: RANDOM FOREST FLAIR RECONSTRUCTION FROM T_1 , T_2 , AND P_D -WEIGHTED MRI. *Proc IEEE Int Symp Biomed Imaging* 2014: 1079-1082, 2014.
76. Ronneberger O, Fischer P and Brox T: U-Net: Convolutional Networks for Biomedical Image Segmentation. *Lect Notes Comput Sci* 9351: 234-241, 2015.

77. Salem M, Valverde S, Cabezas M, Pareto D, Oliver A, Salvi J, Rovira A and Lladó X: Multiple sclerosis lesion synthesis in MRI using an encoder-decoder U-NET. *IEEE Access* 7: 25171-25184, 2019.
78. Wei W, Poirion E, Bodini B, Durrleman S, Ayache N, Stankoff B and Colliot O: Predicting PET-derived demyelination from multimodal MRI using sketcher-refiner adversarial training for multiple sclerosis. *Med Image Anal* 58: 101546, 2019.
79. Finck T, Li H, Grundl L, Eichinger P, Bussas M, Mühlau M, Menze B and Wiestler B: Deep-Learning Generated Synthetic Double Inversion Recovery Images Improve Multiple Sclerosis Lesion Detection. *Invest Radiol* 55: 318-323, 2020.
80. Yoon J, Gong E, Chatnuntawech I, Bilgic B, Lee J, Jung W, Ko J, Jung H, Setsompop K, Zaharchuk G, *et al*: Quantitative susceptibility mapping using deep neural network: QSMnet. *Neuroimage* 179: 199-206, 2018.
81. Bollmann S, Rasmussen KGB, Kristensen M, Blendal RG, Østergaard LR, Plocharski M, O'Brien K, Langkammer C, Janke A and Barth M: DeepQSM-using deep learning to solve the dipole inversion for quantitative susceptibility mapping. *Neuroimage* 195: 373-383, 2019.
82. Dewey BE, Zhao C, Reinhold JC, Carass A, Fitzgerald KC, Sotirchos ES, Saidha S, Oh J, Pham DL, Calabresi PA, *et al*: DeepHarmony: A deep learning approach to contrast harmonization across scanner changes. *Magn Reson Imaging* 64: 160-170, 2019.
83. Liu H, Xiang QS, Tam R, Dvorak AV, MacKay AL, Kolind SH, Traboulsee A, Vavasour IM, Li DKB, Kramer JK, *et al*: Myelin water imaging data analysis in less than one minute. *Neuroimage* 210: 116551, 2020.



This work is licensed under a Creative Commons Attribution-NonCommercial-NoDerivatives 4.0 International (CC BY-NC-ND 4.0) License.